

## DFT Study of Structural and Electronic Properties of PdO/HZSM-5

Jian-guo Wang and Chang-jun Liu\*

ABB Plasma Greenhouse Gas Chemistry Laboratory, Key Laboratory for Green Chemical Technology of Ministry of Education and School of Chemical Engineering, Tianjin University, Tianjin 300072, People's Republic of China

Zhiping Fang, Yue Liu, and Zhongqi Han

Science & Technology Development Center, China Petroleum & Chemical Corporation (SINO-PEC), Beijing 100029, People's Republic of China

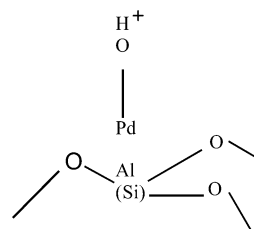
Received: June 23, 2003; In Final Form: November 23, 2003

A density functional theory (DFT) study has been conducted to investigate the structural and electronic properties of PdO/HZSM-5 and thereby the relationship between PdO and the acid sites of HZSM-5. Different cluster models of PdO/HZSM-5 based on experimental and theoretical works are presented. The study shows that the local structure of PdO supported on HZSM-5 is very similar to the four-coordinated square planar structure of bulk PdO. This is consistent with the reported EXAFS analysis in the literature. The average distances between the Pd and the four coordinated oxygen atoms obtained by DFT calculations with different cluster models are close to the reported experimental results. The analysis of the Mulliken population and the electron density difference of the cluster models shows that there exists a charge transfer from the four coordinated oxygen atoms to the Pd. The components of the frontier molecular orbital of these cluster models come mainly from the Pd and the four coordinated oxygen atoms. The DFT study confirms that the acid sites in HZSM-5 keep the PdO well dispersed due to the bond interaction between the acidic proton atom and the oxygen atom of PdO. In addition, after the formation of  $\text{PdOH}^+$ , the acidity of HZSM-5 complex remains high or in some instances increases.

## 1. Introduction

Recently, Pd zeolite supported catalysts, especially, Pd/ZSM-5 and Pd/HZSM-5, have attracted increased attention due to their excellent catalytic activity in methane combustion,<sup>1–5</sup> NO reduction by  $\text{CH}_4$ ,<sup>6–9</sup> and many other reactions.<sup>10,11</sup> Much research has been conducted to investigate the state of Pd and the active sites in the Pd/HZSM-5 catalysts.<sup>8,9,12–21</sup> Two principles are widely accepted: (1) a stable and high level of Pd dispersion is desirable for high catalytic activity,<sup>18</sup> and (2) acid sites in zeolite are necessary for the activation of  $\text{CH}_4$ .<sup>7,17,19</sup> There exists a very close relationship between the highly dispersed Pd species and the acid sites in zeolite. Okumura et al. used EXAFS and XANES to investigate the local structure of Pd supported on ZSM-5.<sup>8,20,21</sup> This study showed that aggregated Pd particles only exist on the outer surface of ZSM-5 since the aggregated particle size is larger than the zeolite pore, whereas the dispersed PdO was located within the ZSM-5 pores. The extent of dispersion is determined by the number of acid sites in the ZSM-5. The interaction is between the basic metal oxide PdO and acid sites in zeolites.<sup>22</sup> Based on these investigations, the local structure of Pd/HZSM-5 ( $\text{Si}/\text{Al}_2 = 24$ ) after oxidation at 773 K was proposed and is shown in Chart 1. The structure of highly dispersed PdO was very similar to that of the bulk PdO, with four oxygen atoms each situated 2.02 Å from the Pd atom.<sup>8</sup> One of the major roles of the acid sites in zeolite is to keep the PdO dispersed. Bell et al. investigated the state of Pd in Pd/HZSM-5 by using infrared and mass spec-

CHART 1: Local Structure of Pd in Pd-ZSM-5 ( $\text{Si}/\text{Al}_2 = 24$ ) Oxidized at 773 K<sup>8,20</sup>



troscopies.<sup>16,17</sup> They suggested that the principal active species is  $\text{Pd}^{2+}$  in  $\text{Z}^-\text{H}^+(\text{PdO})\text{H}^+\text{Z}^-$ , where  $\text{Z}^-$  represents the aluminum site in the zeolite. They thought the two adjacent acid sites were responsible for stabilizing the dispersed PdO.

Many experiments have confirmed an interaction between PdO and the acid sites of HZSM-5.<sup>8,16,17,20,21</sup> The complexity of the system makes it difficult to experimentally obtain a precise description of the actual interactions between the metal atoms and the zeolite framework.<sup>23</sup> At present, quantum chemistry calculations have been widely and successfully applied to investigate the properties of metal cations within zeolites.<sup>23–28</sup> Yakovlev and co-workers analyzed the interaction of a proton with small  $\text{Pd}_4$  and  $\text{Pd}_6$  clusters.<sup>29,30</sup> Harmsen et al. studied the interaction of a Pd atom with a zeolite Brønsted acid site.<sup>31</sup> On the basis of DFT calculations, this study showed that the reduction of  $\text{Pd}^{2+}$  to Pd and  $2\text{H}^+$  is highly exothermic.<sup>31</sup> Rice et al. studied the coordination of a group of divalent metal cations (including  $\text{Pd}^{2+}$ ) to ZSM-5 using gradient-corrected DFT.<sup>32</sup> These investigations focused principally on the interac-

\* To whom correspondence should be addressed. Fax: +86 22 27890078. E-mail: changliu@public.tpt.tj.cn.

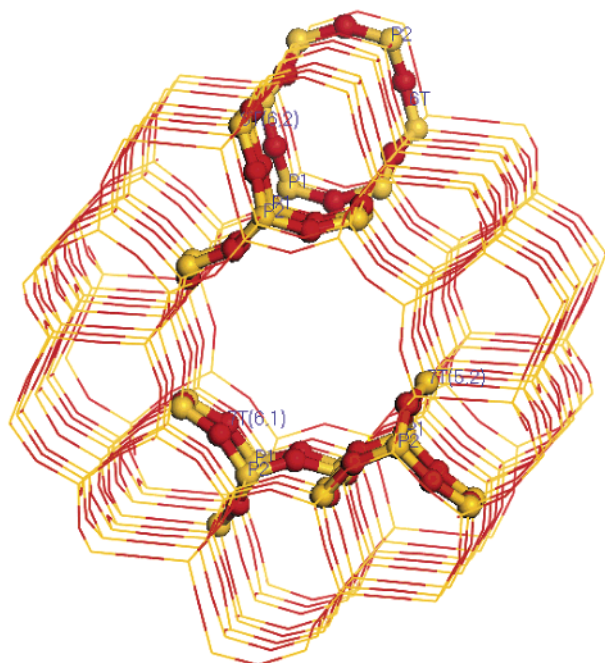


**Figure 1.** Cluster model location in the unit cell of ZSM-5 zeolite.

tion between Pd and HZSM-5. To our knowledge, there has been no theoretical study on the interaction between PdO and HZSM-5.

In the present work, we attempt to understand the structural and electronic properties of PdO/HZSM-5 and the relationship between the highly dispersed PdO and the acid sites of zeolites. The major objectives of this study are (1) to investigate the local structure of PdO/HZSM-5 and compare it with the experimentally determined structure reported in the literature, and further investigate the electronic structure of PdO/HZSM-5; (2) to understand the close relationship between PdO and the acid sites in HZSM-5, and to explain why the acid sites of zeolite can keep the PdO in the dispersed form; and (3) to study the effect of the highly dispersed PdO on the acidity of the catalysts in order to further understand the relationship between the highly dispersed PdO and the acidity of the catalyst, which are two requisites for catalysts with high activity.

## 2. Computational Models and Methods

**Selection of Cluster Models.** Figure 1 shows the location in the ZSM-5 unit cell of the cluster models used in this study. A complete 10-membered ring (10T) is made up of the interconnection of a 5-membered ring (5T) or 6-membered ring (6T). The cluster models (7T(5,2), 7T(6,1), and 8T(6,2)) contain a straight five-, six-, and six-membered-ring structure, as shown in Figure 1. The 6T cluster model represents the deformed six-membered ring at the intersection between the straight and sinusoidal channels.<sup>24</sup> The selection of cluster models was based on previous experimental and theoretical results.<sup>24,29–32</sup> These cluster models best represent the different real geometric environments and the possible metal cation sites.<sup>24</sup> For these clusters, the 7T(6,1) and 6T clusters correspond to the  $\alpha$ - and  $\beta$ -sites of the ZSM-5, which are the metal cation favored sites.<sup>24</sup> The selection of these cluster models is very important for systematically studying the structural and electronic properties of PdO/HZSM-5 and for further understanding the catalytic reaction mechanism. PdO is kept by these cluster models and protrudes toward the outer larger pore. The initial ZSM-5 structure is taken from the siliceous ZSM-5 crystal.<sup>33</sup>

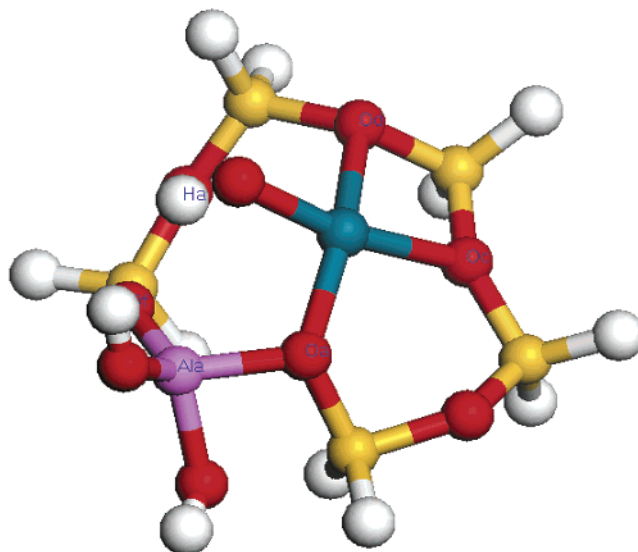


**Figure 2.** Optimized structure of the 6T1Al PdO/HZSM-5 cluster.

In this study, cluster models containing one or two Al atoms were considered in order to investigate the effect of different amounts of Brønsted acid. These cluster models are denoted as 6T1Al, 6T2Al, 7T1Al(5,2), 7T2Al(5,2), 7T1Al(6,1), 7T2Al(6,1), 8T1Al(6,2), and 8T2Al(6,2). Using the Löwenstein rule, the Al position is specified by the P site in Figure 1.<sup>34</sup> The position of Al is P1 when the cluster contains one Al atom, which is shown in Figure 1.

The dangling bond is saturated by OH for the Al atom in all clusters. The Si groups were terminated with H instead of OH in order to avoid intramolecular hydrogen bonds, which would create an unacceptable mode.<sup>35</sup>

**Computational Methods.** All the calculations were performed using the MSI DMol<sup>3</sup> program.<sup>36,37</sup> The double numerical plus polarization (DNP) basis set is used in the calculation to describe the valence orbitals of atoms. The DFT study with DMol<sup>3</sup> was performed with the generalized gradient corrected approximation (GGA) using PW91 functional.<sup>38,39</sup> No symmetry constraints were used for any of the cluster models in this study. The atomic charges were calculated using the approach proposed by Mulliken.<sup>40</sup> The electron density difference and the frontier molecular orbital of the investigated cluster models were also analyzed.

The relative stability of PdO in each framework site is evaluated by calculating the binding energy (BE):

$$E_{\text{bind}} = E(\text{PdO/HZSM-5}) - E(\text{PdO}) - E(\text{HZSM-5})$$

where  $E(\text{PdO/HZSM-5})$ ,  $E(\text{PdO})$ , and  $E(\text{HZSM-5})$  are the electronic energy of the optimized PdO/HZSM-5 cluster, an isolated PdO, and HZSM-5 cluster, respectively.

The deprotonation energy (DE) is used to estimate the acidity of the bridging OH groups, which is expressed as the total energy difference between the initial (neutral) and the deprotonated (anionic) forms of the HZSM-5 or PdO/HZSM-5 clusters. The DE value cannot be directly measured experimentally. The difference between DE values of two different OH groups can be determined from the differences of binding energies of a probe basic molecule.<sup>41</sup>

## 3. Results and Discussion

Figures 2–9 show the optimized structures for the 6T1Al, 6T2Al, 7T1Al(5,2), 7T2Al(5,2), 7T1Al(6,1), 7T2Al(6,1), 8T1Al-

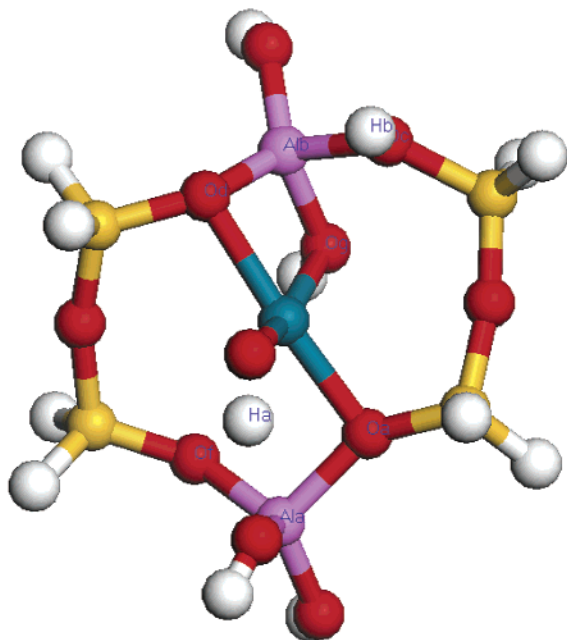


Figure 3. Optimized structure of the 6T2Al PdO/HZSM-5 cluster.

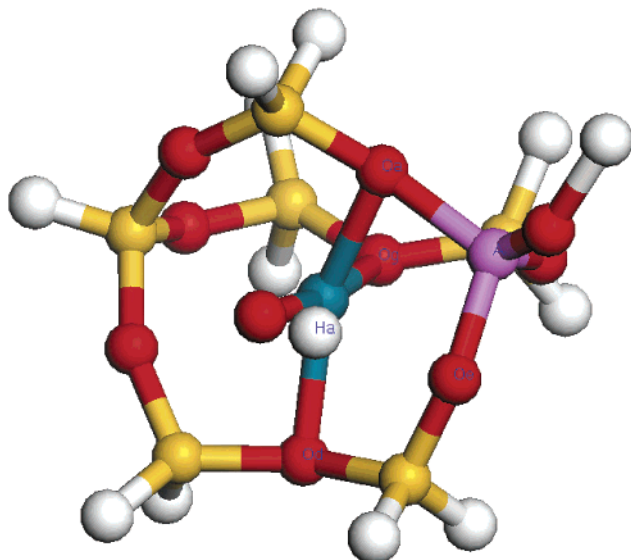


Figure 4. Optimized structure of the 7T1Al(5,2) PdO/HZSM-5 cluster.

(6,2), and 8T2Al(6,2) PdO/HZSM-5 zeolite clusters. The main structural features of the optimized clusters are presented in Table 1.

**Migration and Transfer of Acidic Protons.** For all of the cluster models, the acidic proton Ha migrates toward the oxygen of PdO. Initially in the zeolite, the Of–Ha (or Oe–Ha) bond length is 0.978 Å. After the PdO is introduced into the model, the distance between the Ha and Of (or Oe) is from 2.050 to 4.447 Å for the different cluster models. This shows that there is no bond interaction between Of (or Oe) and Ha. The average bond distance between the PdO oxygen and Ha is 0.983 Å. Evidently, a covalent bond is formed between the Ha and the oxygen atom of PdO. This interaction plays a vital role in making the PdO highly dispersed and keeping the catalytic performance high. For the cluster models containing two Al atoms, the transfer of the acidic proton Hb is less than that of the Ha. For the 6T2Al, 7T2Al(5,2), and 8T2Al(6,2) cluster models, the bond distance of Hb–Oc (or Hb–Ob) is 0.976, 1.081, and 0.979 Å, respectively. The distance between Hb and

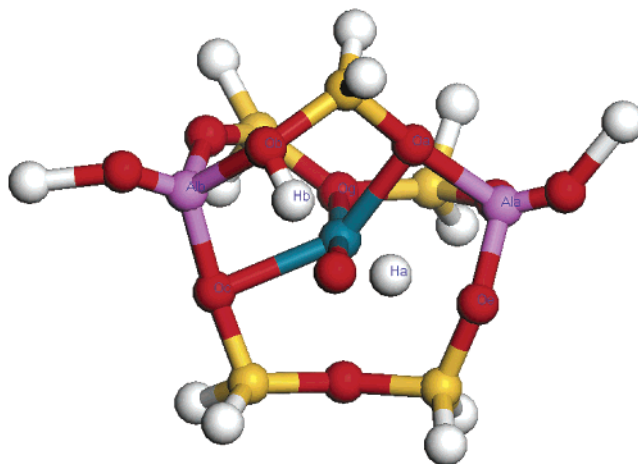


Figure 5. Optimized structure of the 7T2Al(5,2) PdO/HZSM-5 cluster.

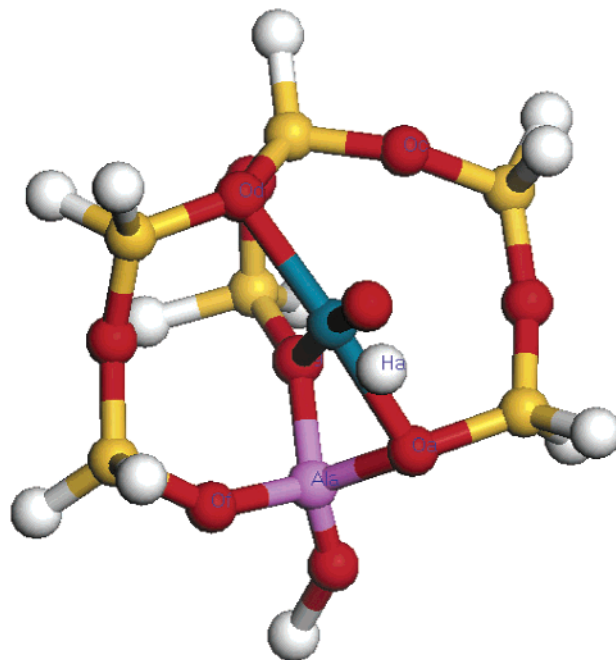


Figure 6. Optimized structure of the 7T1Al(6,1) PdO/HZSM-5 cluster.

the oxygen of PdO is 3.875, 1.442, and 3.130 Å, respectively. The acidic proton Hb undergoes only a minor change, and no strong bond interaction between the Hb and the oxygen atom of PdO is observed for the above-mentioned cluster models. A previous study also showed that the O–H bond length of the remaining bridging OH group changes only very slightly when one of the charge compensating protons was exchanged for a metal cation for two or three Al atom cluster models.<sup>41</sup> For the 7T2Al(6,1) cluster models, the bond distance of O–Ha and O–Hb is 1.004 and 1.005 Å, respectively. The distance of Ha–Of and Hb–Oc is 4.447 and 1.821 Å, respectively.

**Local Structure of PdO/HZSM-5.** The Pd<sup>2+</sup> ion of PdO is considered to be coordinated to a framework oxygen atom if the Pd–O bond distance is shorter than 2.5 Å. For all the cluster models, the Pd–O bond distances ranged from 1.948 to 2.166 Å, which are close to the bulk Pd–O bond distance. This is consistent with the EXAFS results reported by Okumura<sup>8</sup> and Resasco.<sup>14</sup> The distances between Pd and the coordinated framework oxygen atoms are shown in Table 1. It can be seen that the bond distance between Pd and the PdO oxygen atom is shorter than that of Pd with the three coordinated framework oxygen atoms for all the cluster models except the 7T2Al(6,1)



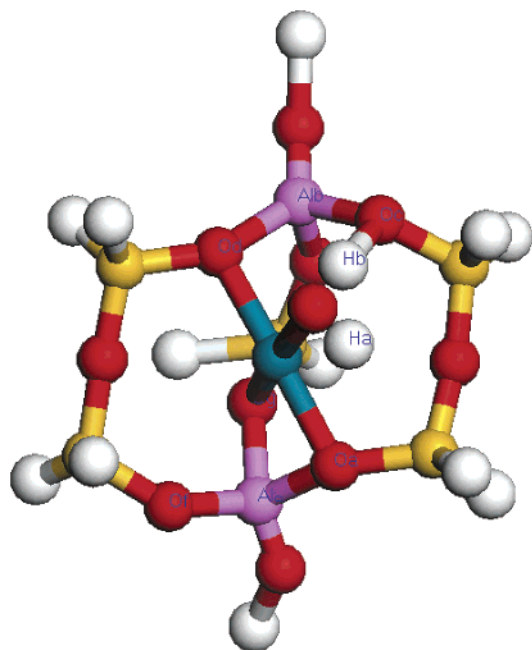


Figure 7. Optimized structure of the 7T2Al(6,1) PdO/HZSM-5 cluster.

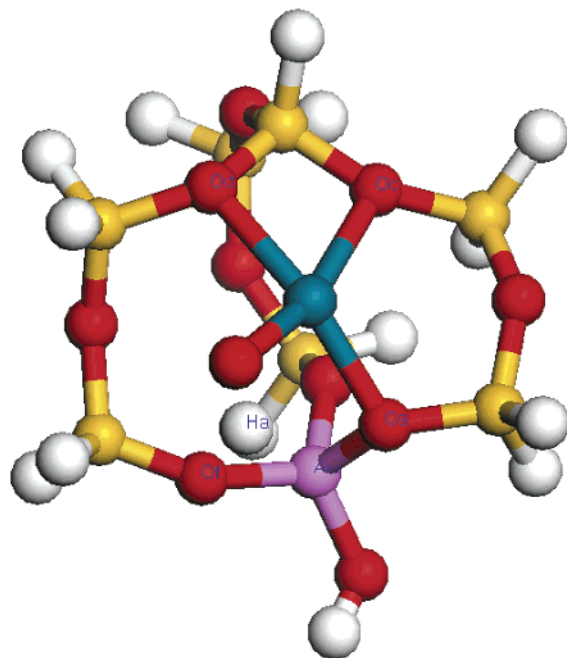


Figure 8. Optimized structure of the 8T1Al(6,2) PdO/HZSM-5 cluster.

(Table 1). This suggests that there is a stronger interaction between Pd and the PdO oxygen atom than between Pd and the three coordinated framework oxygen atoms. Such results cannot be experimentally obtained since the EXAFS can only give the average Pd–O bond distance.<sup>24</sup> This information will be very important for further study of the reaction mechanism. The Pd–O coordination number (CN) and the average Pd–O bond distance obtained from the DFT study and the EXAFS experimental analysis<sup>8,14,20</sup> are shown in Table 2. For all of cluster models, the Oa and Od oxygen (Oc for 7T2Al(5,2)) atoms are both coordinated with Pd. For all of the cluster models in this study, the optimized local structure of Pd with four coordinated oxygen atoms is quite similar to that of the bulk PdO with the four-coordinated square planar structure. Pd and the four coordinated oxygen atoms always tend to keep the same planar distribution, with the Pd atom situated in the center. The

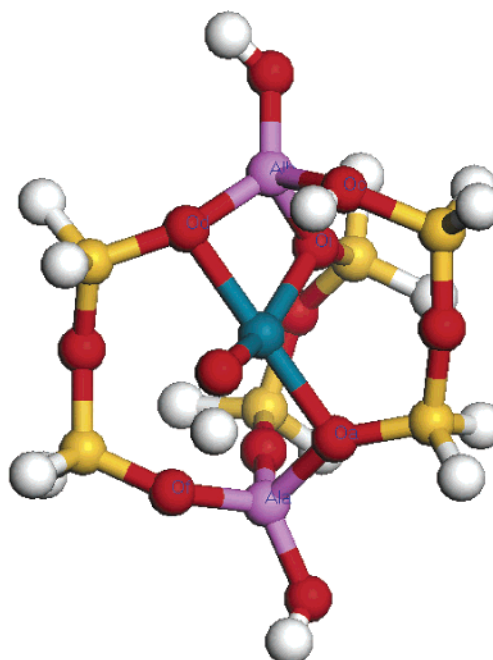


Figure 9. Optimized structure of the 8T2Al(6,2) PdO/HZSM-5 cluster.

local structure of PdO/HZSM-5 determined by the DFT calculations is very consistent with the results obtained from the EXAFS experimental analysis.<sup>8,14,20</sup>

The interaction between Pd and HZSM-5 will cause some changes in the Al–O distance and in the O–Al–O angle. The Al–O distance and the O–Al–O angle are also shown in Table 1. For all cluster models (except Alb–Oc and Alb–Od in 8T2Al(6,2)), the distance between Ala or Alb and the coordinated oxygen is longer than that with the uncoordinated oxygen atom. This can be attributed to the strong interaction between the Pd metal and the coordinated oxygen atom connecting to the Al atom.<sup>25,42</sup> The strong Pd–oxygen (coordinated) interaction weakens the aluminum–oxygen (coordinated with Pd) bond to be elongated.<sup>42</sup> The Of–Ala–Oa (or Oe–Ala–Oa) and Od–Alb–Oc (or Ob–Alb–Oc) angles are also shown in Table 1. It can be seen that the Od–Alb–Oc (or Ob–Alb–Oc) angle is closer to the initial corresponding angle in HZSM-5 than Of–Ala–Oa (or Oe–Ala–Oa). This is consistent with the greater migration of the acidic proton Ha than Hb.

**Electronic Properties of PdO/HZSM-5.** The Mulliken population analysis for Pd, the proton H, and the oxygen atoms (including the coordinated oxygen atoms, oxygen atoms in the Al–O–Si structure, and the oxygen atom in PdO) is presented in Table 3. The calculated Mulliken net charge of Pd is from +0.365 to +0.616 for the different cluster models. These values are far less than the formal charge, +2. The Mulliken charges of the four coordinated oxygen atoms are also shown in Table 3. It can be seen that there is a charge transfer from oxygen to the metal.<sup>25</sup> The charge transfer from zeolite to metal cation enhances the interaction between the zeolite and the metal.<sup>25,43</sup> The charge on the H atom and the oxygen atom of the Brønsted sites can be used to study the acidity.<sup>44–48</sup> A high charge on the H atom corresponds to a high acidity.<sup>44–48</sup> For all cluster models containing two Al atoms, the charge on Hb is higher than that on Ha. This is consistent with previous analysis: the interaction between the oxygen atom of PdO and Ha is stronger than that between the oxygen atom of PdO and Hb.

To better investigate the electronic properties of the clusters, the electron density difference maps are shown in Figure 10.

**TABLE 1: Optimized PdO/HZSM-5 Cluster Properties<sup>a</sup>**

cluster	Pd–O	O–H	O <sub>fra</sub> –H	Pd–O <sub>fra</sub>	Al–O	O–Al–O
6T1Al	1.948	O–Ha 0.981	Ha–Of 2.050	Pd–Oa 2.105 Pd–Oc 2.286 Pd–Od 2.357	Al–Oa 1.844 Al–Of 1.772	Of–Ala–Oa 105.260
6T2Al	1.961	O–Ha 0.991	Ha–Of 3.307	Pd–Oa 2.122 Pd–Od 2.204 Pd–Og 2.277	Ala–Oa 1.866 Ala–Of 1.788 Alb–Oc 1.937 Alb–Od 1.775	Of–Ala–Oa 100.31 Od–Alb–Oc 99.364
7T1Al(6,1)	1.965	O–Ha 0.976	Ha–Of 4.163	Pd–Oa 2.153 Pd–Od 2.221 Pd–Og 2.197	Ala–Oa 1.867 Ala–Of 1.747	Oa–Ala–Of 109.09
7T2Al(6,1)	2.166	O–Ha 1.004	Ha–Of 4.447	Pd–Oa 2.098 Pd–Od 2.075 Pd–Og 2.100	Ala–Oa 1.861 Alb–Od 1.861 Alb–Oc 1.820	Oa–Ala–Of 108.03 Oc–Alb–Od 99.87
7T1Al(5,2)	2.006	O–Ha 0.979	Ha–Oe 2.157	Pd–Oa 2.111 Pd–Od 2.208 Pd–Og 2.210	Ala–Oa 1.928 Ala–Oe 1.823	Oa–Ala–Oe 111.136
7T2Al(5,2)	2.042	O–Ha 0.980	Ha–Oe 2.189	Pd–Oa 2.145 Pd–Oc 2.331 Pd–Og 2.152	Ala–Oa 1.907 Ala–Oe 1.791 Alb–Ob 1.729 Alb–Oc 1.821	Oa–Ala–Oe 104.69 Ob–Alb–Oc 107.79
8T1Al(6,2)	1.974	O–Ha 0.977	Ha–Of 3.082	Pd–Oa 2.098 Pd–Oc 2.139 Pd–Od 2.229	Ala–Oa 1.873 Ala–Of 1.767	Oa–Ala–Of 100.28
8T2Al(6,2)	1.973	O–Ha 0.979	Ha–Of 2.314	Pd–Oa 2.102 Pd–Od 2.161 Pd–Oi 2.312	Ala–Oa 1.879 Ala–Of 1.772 Alb–Oc 1.975 Alb–Od 1.778	Oa–Ala–Of 102.08 Oc–Alb–Od 97.627

<sup>a</sup> All distances are reported in angstroms. The angles are reported in degrees. O represents the oxygen in PdO. O<sub>fra</sub> is denoted as the framework oxygen.

**TABLE 2: Comparison of Coordination Number (CN) and Interatomic Distance between the EXAFS Results and the Average Calculated Results<sup>a</sup>**

	exptl			6T1Al	6T2Al	7T1Al(6,1)	7T2Al(6,1)	7T1Al(5,2)	7T2Al(5,2)	8T1Al(6,2)	8T2Al(6,2)
CN	4 <sup>b</sup>	4 <sup>c</sup>	4 <sup>d</sup>	4	4	4	4	4	4	4	4
Pd–O	2.020	2.009	2.013	2.174	2.141	2.134	2.110	2.134	2.168	2.110	2.137

<sup>a</sup> All the distances are in angstroms. <sup>b</sup> Pd/HZSM-5 (Si/Al<sub>2</sub> = 24).<sup>8</sup> <sup>c</sup> 0.3% Pd/HZSM-5.<sup>14</sup> <sup>d</sup> 1.0% Pd/HZSM-5.<sup>14</sup>

**TABLE 3: Mulliken Population Analysis, Binding Energies, and HOMO–LUMO Gap of PdO with HZSM-5<sup>a</sup>**

	Pd	O			H	BE	HOMO–LUMO gap
6T1Al	0.616	Oa –0.840 Of –0.864	Oc –0.888 O –0.551	Od –0.861	Ha 0.315	69.7415	30.2852
6T2Al	0.522	Oa –0.842 Of –0.839	Oc –0.705 Og –0.660	Od –0.848 O –0.585	Ha 0.327 Hb 0.349	78.5463	32.0084
7T1Al(6,1)	0.534	Oa –0.831 Og –0.863	Od –0.868 O –0.552	Of –0.818	Ha 0.273	72.7878	32.4333
7T2Al(6,1)	0.596	Oa –0.839 Of –0.824	Oc –0.891 Og –0.833	Od –0.859 O –0.462	Ha 0.298 Hb 0.358	98.9482	30.3324
7T1Al(5,2)	0.365	Oa –0.826 Og –0.883	Od –0.851 O –0.546	Oe –0.823	Ha 0.308	45.9088	28.7037
7T2Al(5,2)	0.461	Oa –0.822 Oe –0.850	Ob –0.774 Og –0.880	Oc –0.832 O –0.598	Ha 0.323 Hb 0.410	60.8158	26.7445
8T1Al	0.589	Oa –0.841 Of –0.827	Oc –0.835 O –0.516	Od –0.888	Ha 0.292	62.3032	29.2466
8T2Al	0.560	Oa –0.858 Of –0.851	Oc –0.704 Oi –0.876	Od –0.860 O –0.571	Ha 0.305 Hb 0.363	74.3443	36.1629

<sup>a</sup> All the distances are in angstroms. The BE and HOMO–LUMO gap are in kilocalories per mole.

The most important feature in Figure 10 is the charge transfer from the coordinated oxygen atoms to the palladium. The distribution of electron density difference on the palladium atom shows some directional dependence. The electron density depletion on the Pd atom is more pronounced in these fields near the PdO oxygen and opposite oxygen atom than those near the other zeolite framework oxygen atoms. These results were also confirmed by the Mulliken net charge analysis. The electron density difference on the zeolite framework oxygen atoms is spherical. However, the sphere on the PdO oxygen atom is

distorted due to the effect of the electron density on the hydrogen atom.

The highest occupied molecular orbital (HOMO) and the lowest unoccupied molecular orbital (LUMO) of the investigated cluster were also analyzed in this study. Figure 11 shows the HOMO and LUMO of the 6T2Al PdO/HZSM-5 cluster, as a typical example. It can be seen that the components of the HOMO and LUMO of the 6T2Al PdO/HZSM-5 cluster come mainly from the palladium and the four coordinated oxygen atoms, especially the oxygen atom of palladium oxide. This

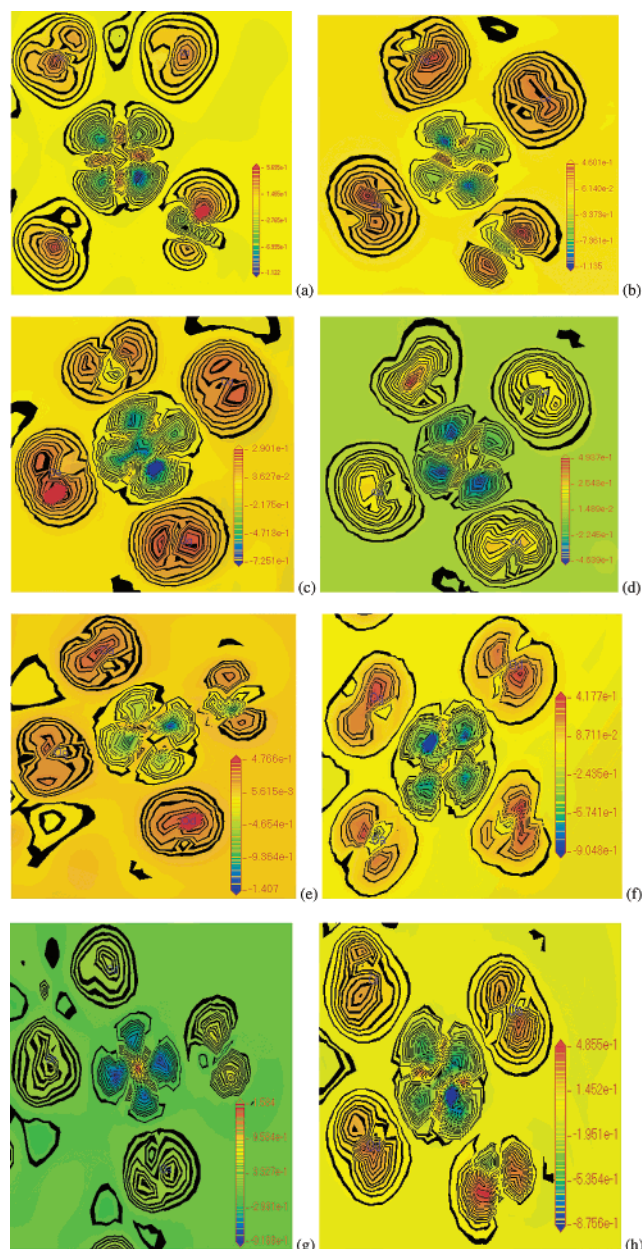


**Figure 10.** Electron density difference maps. (a) 6T1Al PdO/HZSM-5. (b) 6T2Al PdO/HZSM-5. (c) 7T1Al(5,2) PdO/HZSM-5. (d) 7T2Al(5,2) PdO/HZSM-5. (e) 7T1Al(6,1) PdO/HZSM-5. (f) 7T2Al(6,1) PdO/HZSM-5. (g) 8T1Al(6,2) PdO/HZSM-5. (h) 8T2Al(6,2) PdO/HZSM-5.

follows the same rule for the components of HOMO and LUMO as other cluster models. The HOMO–LUMO gap of the cluster models is shown in Table 3.

The BE for PdO of each cluster model is also shown in Table 3. A higher BE value represents a higher stability. By comparing the BE value of PdO in the cluster models containing one or two Al atoms, it can be seen that the stability will increase as the increasing acidity of zeolite. The BE of PdO in HZSM-5, which is less than 100 kcal/mol for all of the cluster models, is smaller than the BE of metal cation ( $\text{Cu}^+$  in ferrierite,<sup>27</sup>  $\text{Cu}^+$  in ZSM-5<sup>49</sup>), which is more than 150 kcal/mol. This is consistent

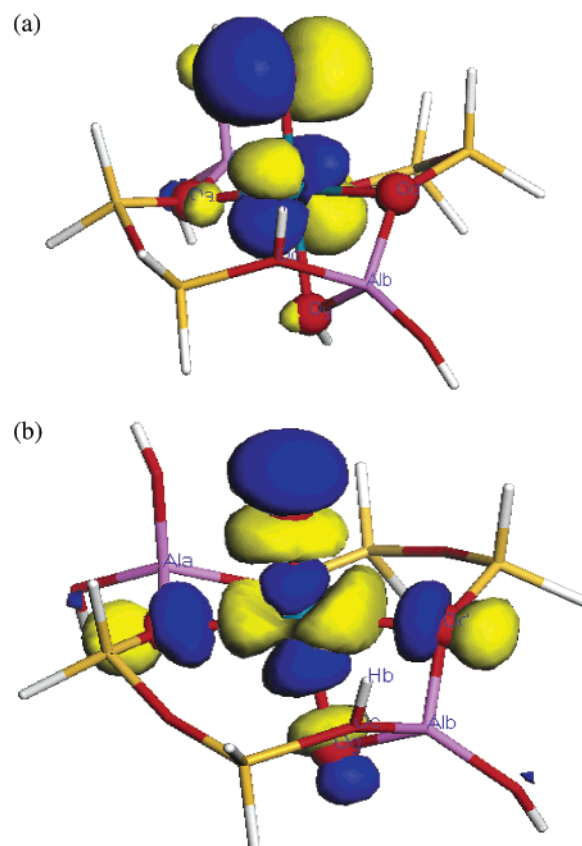


**Figure 11.** HOMO and LUMO of the 6T2Al PdO HZSM-5 cluster. (a) HOMO; (b) LUMO.

with the reported experimental results, where PdO in HZSM-5 has a moderate stability and high mobility.<sup>8</sup>

**Relationship between Dispersed PdO and Acid Sites.** From the above analysis, it can be seen that the acidic proton Ha migrates toward the oxygen atom of PdO. The average bond distance of O–Ha is 0.983 Å. The new bond between Ha and the PdO oxygen atom has been formed after breaking the bond between Ha and the framework oxygen atom. These have been experimentally confirmed.<sup>8,17,20,50</sup> An infrared spectroscopy experiment by Bell and co-workers showed that the PdO species were kept by the Brønsted acid site of zeolite.<sup>17</sup> They denoted the species as  $\text{Z}^-\text{H}^+(\text{PdO})$  or  $\text{Z}^-\text{H}^+(\text{PdO})\text{H}^+\text{Z}^-$ .<sup>17</sup> Different models in this study confirm such conclusions. It can be seen that the PdO species are kept by two Brønsted acid sites of zeolite in the 7T2Al(6,1) model or one Brønsted acid site of zeolite in other models. The EXAFS experiment by Okumura et al. showed that the dispersion of PdO was dependent on the acid amount of ZSM-5 support.<sup>8,20,50</sup> Both the experimental and theoretical studies confirm that there is a close relationship between the highly dispersed PdO and the acid site of HZSM-5. An interaction between the acidic proton and the oxygen atom of PdO can hinder the formation of aggregated PdO and make the PdO more highly dispersed. Highly dispersed PdO is necessary to keep the catalytic activity of PdO/HZSM-5 high. Okumura proposed that the driving force for the dispersion of PdO is the acid–base interaction between the acid sites of the zeolite and the PdO, which has a basic character.<sup>8,20,50</sup> Due to

**TABLE 4: Deprotonation Energy for HZSM-5 and PdO/HZSM-5 Containing Two Al Atoms<sup>a</sup>**

cluster	6T2H	6T2Al	7T2H(6,1)	7T2Al(6,1)	7T2H(5,2)	7T2Al(5,2)	8T2H(6,2)	8T2Al(6,2)
DE	330.211	335.453	299.584	300.1344	303.5324	299.3945	276.8972	278.403

<sup>a</sup> DE is in kilocalories per mole.



the close relationships between the acidity of HZSM-5 and the dispersion of PdO, the dispersion of PdO on HZSM-5 can be regulated by changing the acidity of HZSM-5 with various methods (for example, glow discharge plasma treatment,<sup>3,4</sup> change of the Si/Al ratio in HZSM-5,<sup>50,51</sup> or the addition of a promoter<sup>5</sup>). Thereby the activity and stability of Pd/HZSM-5 can be improved.

It is well-known that the acidity of zeolite is necessary for NO reduction by CH<sub>4</sub>.<sup>7,17,19</sup> Also, the catalytic performance of Pd is highly dependent on the amount of acid amount in ZSM-5.<sup>8</sup> The Pd/HZSM-5 (Si/Al<sub>2</sub> = 24) catalyst, on which the PdO is highly dispersed, has very good catalytic activity. This exhibits that the catalyst has sufficient acid sites. This study shows that the proton (Brønsted acid) can migrate and transfer significantly. To confirm whether the acidity of Pd/HZSM-5 changes, the calculations of DE for HZSM-5 and Pd/HZSM-5 containing two Al atoms have been carried out in this study. It has been shown that the DE can be used as an effective method to evaluate the acidity of zeolite.<sup>41,52–54</sup> The DE values for different cluster models are shown in Table 4. The lower the DE value of an OH group, the higher is its Brønsted acidity.<sup>41</sup> For 7T2Al(5,2) PdO/HZSM-5, the acidity even increases. For most of these cluster models, the PdOH<sup>+</sup> fragment is formed when the acidic proton migrates toward the oxygen atom of the PdO due to covalent bond interaction. Therefore, these cluster models can be considered as one of proton H substituted by PdOH<sup>+</sup>. Some studies have showed that the mixed clusters containing both protons and metal cations (alkali and alkaline earth)<sup>41</sup> or Ca-(OH)<sup>+</sup>, AlO<sup>+</sup>, and Al(OH)<sub>2</sub><sup>+</sup><sup>52</sup> for charge compensation are more acidic than the pure protonic form. Barbosa and van Santen et al. showed that a ZnOH<sup>+</sup> enhanced the acidity of a bridging OH group using the DFT calculation with the two coupled four-ring zeolite cluster.<sup>55</sup> The present study confirms these conclusions.

#### 4. Conclusion

In conclusion, the present DFT study confirms that Pd with four coordinated oxygen atoms over PdO/HZSM-5 always maintains a square planar structure. This is the most stable bulk PdO structure. This is consistent with the reported EXAFS analysis.<sup>8,14</sup> The average distances between the Pd and the four coordinated oxygen atoms obtained by the DFT calculations with different cluster models are close to experimental results.<sup>8,14</sup> The present DFT study also confirms that there is a close relationship between the acid sites of zeolite and PdO, which has also been concluded from EXAFS analyses.<sup>8,14</sup> Because of the bond interaction between the acidic proton and the oxygen atom of PdO which leads to the formation of PdOH<sup>+</sup>, the acid sites of zeolite can make and keep PdO highly dispersed. After the formation of PdOH<sup>+</sup>, the acidity of the catalyst remains high.

**Acknowledgment.** The support from Sino-PEC (under Contract No. X501031) and the National Natural Science Foundation of China (under Contract No. 20225618) is greatly appreciated. The authors also thank Dr. Jeanne Wynn in the Department of Chemistry of Tianjin University for her excellent job in correcting the use of English.

#### References and Notes

- (1) Okumura, K.; Matsumoto, S.; Nishiaki, N.; Niwa, M. *Appl. Catal. B* **2003**, *40*, 151.
- (2) Gélin, P.; Primet, M. *Appl. Catal. B* **2002**, *39*, 1.
- (3) Liu, C.-J.; Yu, K.-L.; Zhu, X.-L.; Zhang, Y.-P.; He, F.; Eliasson, B. Characterization of Plasma Treated Pd/HZSM-5 Catalyst for Methane Combustion. *Appl. Catal. B* **2004**, *47*, 95.
- (4) Liu, C.-J.; Yu, K.-L.; Zhang, Y.-P.; Zhu, X.; He, F.; Eliasson, B. *Catal. Commun.* **2003**, *4*, 303.
- (5) Shi, C.-K.; Yang, L.-F.; Wang, Z.-C.; He, Xiang.-E.; Cai, J.-X.; Li, G.; Wang, X.-S. *Appl. Catal. A* **2003**, *243*, 379.
- (6) Nishizaka, Y.; Misono, M. *Chem. Lett.* **1993**, 1295.
- (7) Nishizaka, Y.; Misono, M. *Chem. Lett.* **1994**, 2237.
- (8) Okumura, K.; Amano, J.; Yasunobu, N.; Niwa, M. *J. Phys. Chem. B* **2000**, *104*, 1050.
- (9) Wen, B.; Sun, Q.; Sachtler, W. M. H. *J. Catal.* **2001**, *204*, 314.
- (10) Bi, Y. S.; Liu, J. F.; Lu, G. X. *Acta Chim. Sin.* **2002**, *60*, 1624.
- (11) Dams, M.; Drijkoningen, L.; Pauwels, B.; van Tendeloo, G.; de Vos, D. E.; Jacobs, P. A. *J. Catal.* **2002**, *209*, 225.
- (12) Descorme, C.; Gélin, P.; Lécuyer, C.; Primet, M. *J. Catal.* **1998**, *177*, 352.
- (13) Ogura, M.; Hayashi, M.; Kikuchi, E. *Catal. Today* **1998**, *45*, 139.
- (14) Ali, A.; Alvarez, W.; Loughran, C. J.; Resasco, D. E. *Appl. Catal. B* **1997**, *14*, 13.
- (15) Adelman, B. J.; Sachtler, W. M. H. *Appl. Catal. B* **1997**, *14*, 1.
- (16) Lobree L. J.; Aylor, A. W.; Reimer, J. A.; Bell, A. T. *J. Catal.* **1999**, *181*, 189.
- (17) Aylor, A. W.; Lobree, L. J.; Reimer, J. A.; Bell, A. T. *J. Catal.* **1997**, *172*, 453.
- (18) Wen, B.; Jia, J.; Sachtler, W. M. H. *J. Phys. Chem. B* **2002**, *106*, 7520.
- (19) Loughran, C. J.; Sachtler, W. M. H. *Appl. Catal. B* **1995**, *7*, 113.
- (20) Okumura, K.; Amano, J.; Niwa, M. *Chem. Lett.* **1999**, 997.
- (21) Okumura, K.; Niwa, M. *Top. Catal.* **2002**, *18*, 85.
- (22) Sanderson, R. T. *Inorganic Chemistry*; Reinhold Publishing Corp.: New York, 1967.
- (23) Shubin, A. A.; Zhidomirov, G. M.; Yakovlev, A.; van Santen, R. A. *J. Phys. Chem. B* **2001**, *105*, 4928.
- (24) Wichterlová, B.; Sobalík, Z.; Dědeček, J. *Appl. Catal. B* **2003**, *41*, 97.
- (25) Šponer, J. E.; Sobalík, Z.; Leszczynski, J.; Wichterlová, B. *J. Phys. Chem. B* **2001**, *105*, 8285.
- (26) Berthomieu, D.; Ducéré, J.-M.; Goursot, A. *J. Phys. Chem. B* **2002**, *106*, 7483.
- (27) Nachtigall, P.; Davidová, M.; Nachtigallová, D. *J. Phys. Chem. B* **2001**, *105*, 3510.
- (28) Rice, M. J.; Chakraborty, A. K.; Bell, A. T. *J. Phys. Chem. A* **1998**, *102*, 7498.
- (29) Yakovlev, A. L.; Zhidomirov, G. M.; Rösch, N. *J. Phys. Chem.* **1996**, *100*, 3482.
- (30) Yakovlev, A. L.; Zhidomirov, G. M.; Neyman, K. M.; Nasluzov, V. A.; Rösch, N. *Ber. Bunsen-Ges. Phys. Chem.* **1996**, *100*, 413.
- (31) Harmsen, R.; Bates, S.; van Santen, R. A. *Faraday Discuss.* **1997**, *106*, 443.
- (32) Rice, M. J.; Chakraborty, A. K.; Bell, A. T. *J. Phys. Chem. B* **2000**, *104*, 9987.
- (33) *Materials Studio*, Version 2.2; Accelrys Inc.: San Diego, 2002.
- (34) Löwenstein, W. *Am. Mineral.* **1954**, *39*, 92.
- (35) Sauer, J.; Ugliengo, P.; Garrone, E.; Saunders, V. R. *Chem. Rev.* **1994**, *94*, 2095.
- (36) Delley, B. *J. Chem. Phys.* **1990**, *92*, 508.
- (37) Delley, B. *J. Chem. Phys.* **2000**, *113*, 7756.
- (38) Perdew, J. P.; Wang, Y. *Phys. Rev. B* **1992**, *45*, 13244.
- (39) Perdew, J. P.; Wang, Y. *Phys. Rev. B* **1986**, *33*, 8800.
- (40) Mulliken, R. S. *J. Chem. Phys.* **1955**, *23*, 1833.
- (41) Vayssilov, G. N.; Rösch, N. *J. Phys. Chem. B* **2001**, *105*, 4277.
- (42) Koningsderger, D. C.; Miller, J. T. *Stud. Surf. Sci. Catal.* **1995**, *97*, 125.
- (43) Berthomieu, D.; Krishnamurty, S.; Coq, B.; Delahay, G.; Goursot, A. *J. Phys. Chem. B* **2001**, *105*, 1149.
- (44) Fripiat, J. G.; Galet, P.; Delhalle, J.; Andre, J. M.; Nagy, J. M.; Derouane, E. G. *J. Phys. Chem.* **1985**, *89*, 1932.
- (45) Beran, S. *J. Phys. Chem.* **1990**, *94*, 335.
- (46) Kramer, G. J.; van Santen, R. A. *J. Am. Chem. Soc.* **1993**, *115*, 2887.
- (47) Soscun, H.; Hernandez, J.; Castellano, O.; Diaz, G.; Hinchliffe, A. *Int. J. Quantum Chem.* **1998**, *70*, 951.
- (48) Tielens, F.; Langenaeker, W.; Geelings, P. *J. Mol. Struct. (THEOCHEM)* **2000**, *496*, 153.
- (49) Treesukol, P.; Limtrakul, J.; Truong, T. N. *J. Phys. Chem. B* **2001**, *105*, 2421.
- (50) Okumura, K.; Niwa, M. *J. Phys. Chem. B* **2000**, *104*, 9670.
- (51) Descorme, C.; Gélin, P.; Lécuyer, C.; Primet, M. *Appl. Catal. B* **1997**, *13*, 185.
- (52) Gonzales, N.; Chakraborty, A. K.; Bell, A. T. *Catal. Lett.* **1998**, *50*, 135.
- (53) Sierka, M.; Eichler, U.; Datka, J.; Sauer, J. *J. Phys. Chem. B* **1998**, *102*, 6397.
- (54) Gonzales, N.; Bell, A. T.; Chakraborty, A. K. *J. Phys. Chem. B* **1997**, *101*, 10058.
- (55) Barbosa, L. A. M. M.; van Santen, R. A. *Catal. Lett.* **1997**, *63*, 97.